INTERNATIONAL JOURNAL FOR NUMERICAL METHODS IN ENGINEERING
Int. J. Numer. Meth. Engng 2012; **89**:227–240
Published online 20 July 2011 in Wiley Online Library (wileyonlinelibrary.com). DOI: 10.1002/nme.3241

A novel numerical method of high-order accuracy for flow in unsaturated porous media

C. E. Zambra[1,*,†], M. Dumbser[2], E. F. Toro[2] and N. O. Moraga[3]

[1] *Universidad Arturo Prat, Centro de Investigación y Desarrollo de Recursos Hídricos (CIDERH), Av. Arturo Prat 2120, Iquique, Chile*
[2] *Laboratory of Applied Mathematics, University of Trento, Via Mesiano 77, I-38100 Trento, Italy*
[3] *Departamento de Ingeniería Mecánica, Universidad de La Serena, Benavente 980, La Serena, Chile*

SUMMARY

We construct finite volume schemes of very high order of accuracy in space and time for solving the nonlinear *Richards* equation (RE). The general scheme is based on a three-stage predictor–corrector procedure. First, a high-order weighted essentially non-oscillatory (WENO) reconstruction procedure is applied to the cell averages at the current time level to guarantee monotonicity in the presence of steep gradients. Second, the temporal evolution of the WENO reconstruction polynomials is computed in a predictor stage by using a global weak form of the governing equations. A *global* space–time DG FEM is used to obtain a scheme without the parabolic time-step restriction caused by the presence of the diffusion term in the RE. The resulting nonlinear algebraic system is solved by a Newton–Krylov method, where the generalized minimal residual method algorithm of Saad and Schulz is used to solve the linear subsystems. Finally, as a third step, the cell averages of the finite volume method are updated using a one-step scheme, on the basis of the solution calculated previously in the space–time predictor stage. Our scheme is validated against analytical, experimental, and other numerical reference solutions in four test cases. A numerical convergence study performed allows us to show that the proposed novel scheme is high order accurate in space and time. Copyright © 2011 John Wiley & Sons, Ltd.

Received 29 September 2010; Revised 30 March 2011; Accepted 6 May 2011

KEY WORDS: unsaturated porous media; soil water transport; novel numerical method; ADER schemes; space–time DG method

1. INTRODUCTION

1.1. Flow in unsaturated porous media

Prediction of water movement in unsaturated porous media is commonly based on the classical Richards equation (RE) [1],

$$\frac{\partial \theta(h)}{\partial t} = \frac{\partial}{\partial x}\left[K(h)\frac{\partial h}{\partial x} - K(h)\right] - S(h), \tag{1}$$

where θ is the water content, h is the hydraulic pressure or pressure head, K is the hydraulic conductivity, t is time, x is the spatial variable in the porous medium, and S is a sink term. Equation (1) is solved for the field $h(x,t)$. This second-order nonlinear PDE for water flow provides mixed parabolic–elliptic behavior under conditions of variable water saturation of the soil. Parabolic behavior occurs in unsaturated media, and elliptic behavior occurs during saturation [2]. The RE is a highly nonlinear PDE because both the hydraulic conductivity $K(h)$ and the water content $\theta(h)$ are highly

*Correspondence to: C. E. Zambra, Universidad Arturo Prat, Centro de Investigación y Desarrollo de Recursos Hídricos (CIDERH), Av. Arturo Prat 2120, Iquique, Chile.
†E-mail: carlos.zambra.s@gmail.com

nonlinear functions of the pressure head h. The form (1) of RE is generally considered superior to other forms of this equation because of its robustness with respect to mass balance [2–4]. Actually, as it is written in a flux–divergence form, Equation (1) has *conservation-law form* with a source term, for the water content θ.

Numerical solution of RE by current schemes generally decouples the issues of temporal and spatial discretization. The time discretization is typically based on the backward Euler scheme [5, 6]. Other time-stepping schemes used for RE include the Crank–Nicholson scheme, the three-level Lees scheme, the Douglas–Jones predictor–corrector method, implicit Runge–Kutta schemes, and backward difference formulae. An adaptive step-size, variable-order, backward difference formulae for the time derivative together with an LDG method for the discretization of the diffusion term has been developed by Li *et al*. [7, 8]. The spatial discretization of RE is commonly performed by using finite element or finite difference methods. Mass lumping is employed to improve the numerical stability and efficiency of the finite element models as previous findings indicate that a consistent mass formulation can cause spurious oscillations [3, 4, 9]. An efficient finite volume discretization on unstructured meshes has been implemented by McBride *et al*. [10]. The finite volume method for diffusion problems on unstructured meshes is extended to the nonlinear RE through Kirchoff transformation, and convergence is theoretically proved in the Reference [11]. In Reference [12], the mass conservative approach developed by Celia *et al*. [4] is extended to a cell-centered version of the finite volume method based on vertex reconstruction. The nonlinear algebraic systems that arise from the implicit discretizations of RE may be solved with iterative schemes, such as, the Picard method, Newton iteration methods, or fast secant methods. In most of these approaches, the nonlinear problem is accounted for by solving a sequence of linear sub-problems, in particular in the Newton method. The linear sub-problems are usually also solved with iterative methods, such as over-relaxed Jacobi, over-relaxed Gauss–Seidel, pre-conditioned CG, biconjugate gradient stabilized method, and generalized minimal residual (GMRES) method [13]. Non-iterative methods, such as the implicit factored scheme, have also been proposed to solve the nonlinearities in RE [14–16].

1.2. The hydraulic properties of unsaturated soil

Relationships between pressure head and water content or pressure head and hydraulic conductivity have been reported by several authors by proposing predictive models [17–22]. The most common models employed by the community and also used in this work are described in the succeeding paragraphs, namely, the van Genuchten model [18] and the predictive model of Mualem [23].

The model for the relative hydraulic conductivity function, $K_{\mathrm{r}}(h)$, can be written in the form

$$K_{\mathrm{r}}(S_{\mathrm{e}}(h)) = S_{\mathrm{e}}^{l}\left(\int_0^{S_{\mathrm{e}}} \frac{\mathrm{d}x}{h(x,t)}\right)^2 \left(\int_0^1 \frac{\mathrm{d}x}{h(x,t)}\right)^{-2}, \qquad K_{\mathrm{r}} = K/K_{\mathrm{s}}, \tag{2}$$

in which K is the unsaturated hydraulic conductivity, K_{s} is the saturated hydraulic conductivity, l is the pore connectivity parameter, usually assumed to be 0.5, and S_{e} is the effective saturation obtained from the equation

$$S_{\mathrm{e}}(h) = \frac{\theta(h) - \theta_{\mathrm{r}}}{\theta_{\mathrm{s}} - \theta_{\mathrm{r}}}. \tag{3}$$

Here θ is the volumetric water content, and θ_{r} and θ_{s} are the residual and saturated water contents, respectively. For the water content of the pressure head function (water retention curve), van Genuchten [18] proposed the following equation:

$$\theta(h) = \begin{cases} \theta_{\mathrm{r}} + \dfrac{\theta_{\mathrm{s}} - \theta_{\mathrm{r}}}{[1 + |\alpha h|^n]^m} & \text{if } h < 0, \\ \theta_{\mathrm{s}} & \text{if } h \geqslant 0. \end{cases} \tag{4}$$

DOI: 10.1002/nme

Equation (2) leads to the following equation for the unsaturated hydraulic conductivity

$$K(h) = \begin{cases} K_s K_r(h) & \text{if } h < 0, \\ K_s & \text{if } h \geqslant 0, \end{cases} \tag{5}$$

with

$$K_r(S_e) = S_e^l \left[1 - (1 - S_e^{1/m})^m\right]^2. \tag{6}$$

Here n and m are empirical shape parameters and $m = 1 - 1/n$. A second model used in this work is called the *Brooks–Corey* model [17], in which the hydraulic conductivity and water content are obtained as follows:

$$K = K_s (S_e)^\eta \tag{7}$$

$$\theta = \begin{cases} \theta_r + (\theta_s - \theta_r)\,(h/h_d)^{-n} & \text{if } h < h_d, \\ \theta_s & \text{if } h \geqslant h_d. \end{cases} \tag{8}$$

In this model, η is a soil parameter and $h_d = -1/\alpha$; here α is an empirical parameter.

In Section 2, our high-order one-step weighted essentially non-oscillatory (WENO) finite volume scheme for RE is described. In particular, a new WENO procedure is outlined in Section 2.2, and the global space–time Galerkin predictor used is presented in Section 2.3. In Section 3, the convergence studies for the schemes developed in the previous section are presented. In Section 4, numerical results obtained with the proposed three-stage predictor–corrector procedure are compared with either exact or finite method solutions in four test cases. Finally, the main conclusions are summarized in Section 5.

2. A HIGH-ORDER FULLY DISCRETE FINITE VOLUME SCHEME FOR RICHARDS EQUATION

In this article, we propose to solve RE by a new fully discrete WENO finite volume scheme with high order of accuracy in space and time. As the finite volume framework only evolves cell averages of the conserved quantity, high order in space is obtained by applying a spatial reconstruction operator to the cell averages. Second, these reconstruction polynomials are evolved in time, as in the original essentially non-oscillatory (ENO) method of Harten *et al*. [24] or in the latest variant of the accuracy derivate (ADER) schemes proposed by Dumbser *et al*. [25, 26]. Whereas the time discretization of the original ADER method, introduced by Toro and Titarev [27] and Titarev and Toro [28], was based on the solution of the generalized Riemann problem (GRP) and the strong differential form of the governing PDE, the new approach of Dumbser *et al*. uses a weak integral formulation of the governing PDE in space–time. However, to avoid the parabolic time-step restriction inherent to explicit schemes, in this article, we propose to use a globally implicit predictor, given by the space–time DG scheme of van der Vegt and van der Ven [29, 30]. The result of the predictor is then used in a fully discrete one-step finite volume scheme in order to compute the inter-cell fluxes.

2.1. *Finite volume schemes for nonlinear Richards equation*

Richards equations (1) can be expressed under the general form of a balance law with source term as

$$\begin{cases} \text{PDE:} & \dfrac{\partial}{\partial t}\theta(h) + \nabla \cdot f(h, \nabla h) = S(h), \\ \text{IC:} & h(x, 0) = h_0(x), \end{cases} \tag{9}$$

with flux

$$f(h) = -K(h)\,(h_x - 1)\,. \tag{10}$$

DOI: 10.1002/nme

The computational domain is divided into a set of non-overlapping spatial control volumes $Q_i = \left[x_{i-\frac{1}{2}}; x_{i+\frac{1}{2}}\right]$ of mesh size $\Delta x = x_{i+\frac{1}{2}} - x_{i-\frac{1}{2}}$, and the time step is denoted by $\Delta t = t^{n+1} - t^n$. Integrating (9) over a finite space–time control volume $\left[x_{i-\frac{1}{2}}; x_{i+\frac{1}{2}}\right] \times [t^n; t^{n+1}]$, we obtained the following finite volume formulation of RE:

$$\bar{\theta}_i^{n+1} = \bar{\theta}_i^n - \frac{\Delta t}{\Delta x}\left[f_{i+\frac{1}{2}} - f_{i-\frac{1}{2}}\right] + \Delta t \overline{S}_i, \tag{11}$$

where the cell average of the water content at time t^n is defined as

$$\overline{\theta}_i^n = \frac{1}{\Delta x_i}\int_{x_{i-\frac{1}{2}}}^{x_{i+\frac{1}{2}}} \theta(h(x,t^n))\mathrm{d}x. \tag{12}$$

The integration of PDE (9) in space and time gives rise to temporal integrals of the fluxes across the element boundaries $f_{i+\frac{1}{2}}$ and the space–time integral of the source term $\bar{S}_i$, which are defined as follows:

$$f_{i+\frac{1}{2}} = \frac{1}{\Delta t}\int_{t^n}^{t^{n+1}} \mathcal{G}_{i\pm\frac{1}{2}}\left(h\left(x_{i+\frac{1}{2}}^-, t\right), h\left(x_{i+\frac{1}{2}}^+, t\right)\right)\mathrm{d}t, \quad \overline{S_i} = \frac{1}{\Delta x \Delta t}\int_{t^n}^{t^{n+1}}\int_{x_{i-\frac{1}{2}}}^{x_{i+\frac{1}{2}}} S(h(x,t))\mathrm{d}x\mathrm{d}t, \tag{13}$$

where $\mathcal{G}_{i\pm\frac{1}{2}}\left(h\left(x_{i+\frac{1}{2}}^-, t\right), h\left(x_{i+\frac{1}{2}}^+, t\right)\right)$ denotes a numerical flux function (Riemann solver) that depends on the two arguments $h\left(x_{i+\frac{1}{2}}^-, t\right)$ and $h\left(x_{i+\frac{1}{2}}^+, t\right)$, which are the boundary extrapolated values on the left-hand and right-hand side of the element interface $x_{i+\frac{1}{2}}$, respectively.

We note that relation (11) is *exact* if the related integrals are all exact. However, numerical use of the finite volume formula relies on approximations to fluxes and sources, resulting in an approximate formula to cell averages.

The numerical scheme is fully defined when a choice of a particular scheme is made to compute the integral required in order to evaluate the fluxes $f_{i\pm\frac{1}{2}}$ at the cell interfaces. In the last three decades, powerful numerical procedures to calculate fluxes have been proposed to solve hyperbolic equations, for example the fluxes of Godunov [31], Osher [32], and Roe [33] as well as various fluxes based on the approximated Riemann solver of Harten *et al*. [34] (see, e.g., [35–38]). In this paper, we use the viscous Rusanov-type flux proposed in [39] and given explicitly later by Equation (21) as the scheme used in the computations for the test cases analyzed.

The proposed method is an extension to RE of the fully discrete ADER approach. In the ADER approach [27, 28, 38, 40, 41], numerical fluxes are computed from the solution of the GRP (also called high-order Riemann problem) at each interface. This is the Cauchy problem in which the initial conditions on either side of the interface are piecewise smooth functions, piecewise polynomials of arbitrary degree, for example. The original ENO scheme of Harten *et al*. [34] and the ADER scheme of Toro and Titarev [27] have two properties in common: time evolution via Taylor series expansion and use of the Cauchy–Kowalewski procedure to convert time derivatives to spatial derivatives. However, these two methods differ in various aspects. For example, the ADER method develops the full series solution right at the interface, and the solution procedure involves solutions of classical Riemann problems for spatial derivatives at the interface. In addition, the ADER method [27] includes (non-stiff) source terms in the high-order Riemann problem. However, this version of the ADER approach is not able to handle stiff source terms. Therefore, a new class of finite volume schemes of arbitrary accuracy in space and time has been proposed by Dumbser *et al*. [25] for stiff hyperbolic balance laws. In the time-evolution part of algorithm, the Cauchy–Kowalewski procedure is replaced by a local space–time discontinuous Galerkin finite elements scheme to handle the stiff source terms. DG methods have recently received significant attention and are applied to a wide range of hyperbolic and parabolic problems [42–45]. Global space–time DG (GSTDG) schemes are discussed in [29, 30, 46, 47].

DOI: 10.1002/nme

We emphasize that formula (11) together with (13) allows the construction of *arbitrary* high-order accurate finite volume schemes, provided that the approximate solution $h(x,t)$ is high order accurate in space and time. The question is only how to obtain a high-order predictor solution for $h = h(x,t)$ in space and time. As (11) only computes the time update of the cell averages for the water content $\bar{\theta}_i^n$ from time t^n to time t^{n+1}, we need to reconstruct higher-order polynomial data from these cell averages $\bar{\theta}_i^n$ in order to obtain better estimates for the arguments of the flux function and the source terms in the integrals appearing in (13).

Therefore, as described in detail in the subsequent sections, the necessary steps to construct an arbitrary high-order ENO explicit one-step finite volume scheme are the following:

1. Nonlinear (non-oscillatory) WENO reconstruction of spatial polynomials $w_h^n(x)$ from the given cell averages $\bar{\theta}_i^n$ of the water content at time t^n. In short notation: compute $w_h^n(x) = \mathcal{R}\left(\bar{\theta}^n\right)$, where $\mathcal{R}$ denotes the reconstruction operator.
2. Global weak formulation in space–time of the IVP (9), where the initial data are given by the spatial reconstruction polynomial $w_h^n(x)$ for the water content θ at time t^n. This yields a weak solution of (9) for $h(x,t)$ in space–time. In short-hand notation, compute $h(x,t) = \mathcal{E}\left(w_h^n(x)\right)$, where $\mathcal{E}$ denotes the evolution operator.
3. Numerical integration of the integrals in (13) and update of the cell averages according to (11), that is, compute $\bar{\theta}^{n+1} = \bar{\theta}^n + \mathcal{FV}(h(x,t))$, where $\mathcal{FV}$ is an abbreviation for the finite volume scheme given in (11).

2.2. *Nonlinear reconstruction technique*

In this section, we briefly discuss the proposed nonlinear WENO reconstruction procedure to reconstruct higher-order polynomial data within each spatial cell Q_i at time t^n from the given cell averages $\bar{\theta}_i^n$. This corresponds to step (1), as outlined at the end of the previous section. We emphasize already at this point that the reconstruction procedure is *nonlinear* and depends strongly on the input data $\bar{\theta}_i^n$. Thus, the resulting numerical scheme, even when applied to a completely linear PDE, will be nonlinear, and thus, it will not be possible to give a closed expression for the proposed scheme. The reconstruction procedure described here for the one-dimensional (1D) case follows directly from the guidelines given in [48] for general unstructured two-dimensional (2D) and three-dimensional (3D) meshes and summarized in one space dimension in [25]. It reconstructs *entire polynomials*, as the original ENO approach proposed by Harten *et al.* in [24]. However, we formally write our method like a WENO scheme [49, 50]. The most important difference of our approach compared with classical WENO schemes is that standard WENO methods reconstruct *point values* at the Gaussian integration points instead of an entire polynomial valid inside each element Q_i.

2.3. *The global space–time DG predictor*

In order to avoid a parabolic time-step restriction ($\Delta t \propto \Delta x^2$) we do *not* use the local space–time predictor introduced for stiff hyperbolic balance laws in [25] and applied to viscous PDE in [39]. Instead, we use the classical GSTDG method of van der Vegt and van der Ven [29, 30], which is globally implicit and unconditionally stable, as shown in the previously mentioned references. The space of basis and test functions V_h of the GSTDG scheme is chosen to be the space spanned by piecewise space–time polynomials $\phi_k = \phi_k(x,t)$ of degree M.

In the following, we will use the three scalar products of two functions $f(\xi,\tau)$ and $g(\xi,\tau)$:

$$\langle f,g\rangle_{Q_i} = \int_{t^n}^{t^{n+1}} \int_{Q_i} f(x,t)g(x,t)\mathrm{d}x\mathrm{d}t, \quad [f,g]_{Q_i}^t = \int_{Q_i} f(x,t)g(x,t)\mathrm{d}x,$$
$$\{f,g\}_{\partial Q_i} = \int_{t^n}^{t^{n+1}} \int_{\partial Q_i} f(x,t)g(x,t)\mathrm{d}S\mathrm{d}t, \tag{14}$$

DOI: 10.1002/nme

where the first one denotes the space–time scalar product over the space–time element $Q_i \times [t^n; t^{n+1}]$, the second one is the spatial scalar product over the spatial element Q_i, and the third one is the space–time scalar product over the element boundary, $\partial Q_i \times [t^n; t^{n+1}]$. The numerical solution $h(x,t)$ for the hydraulic pressure inside each space–time element is approximated by

$$h_i = h_i(x,t) = \sum_{l=1}^{N^d} \phi_l(x,t)\hat{h}_l^i := \Phi_l \hat{h}_l^i, \tag{15}$$

and the same approach is also used for the water content

$$\theta_i = \theta_i(x,t) = \Phi_l(x,t)\hat{\theta}_l^i, \qquad \text{with} \qquad \hat{\theta}_l^i = \theta\left(\hat{h}_l^i\right), \tag{16}$$

for the flux

$$f_i = f_i(x,t) = \Phi_l(x,t)\hat{f}_l^i, \qquad \text{with} \qquad \hat{f}_l^i = f\left(\hat{h}_l^i, \widehat{\nabla h}_l^i\right), \tag{17}$$

and for the source term

$$S_i = S_i(x,t) = \Phi_l(x,t)\hat{S}_l^i, \qquad \text{with} \qquad \hat{S}_l^i = S\left(\hat{h}_l^i\right). \tag{18}$$

We use the Einstein summation convention that implies summation over all indices appearing twice. Multiplication of the PDE (9) with test functions $\Phi_k \in V_h$ and integration over a space–time element $Q_i \times [t^n; t^{n+1}]$ yields

$$\left\langle \Phi_k, \frac{\partial}{\partial t}\theta_i \right\rangle_{Q_i} + \langle \Phi_k, \nabla f_i \rangle_{Q_i} = \langle \Phi_k, S_i \rangle_{Q_i}. \tag{19}$$

Integrating the first term by parts in time and the second term by parts in space yields the following globally coupled algebraic system for the unknown space–time polynomials $h_i(x,t)$:

$$\begin{aligned} &\left([\Phi_k, \theta(h_i)]_{Q_i}^{t^{n+1}} - \left\langle \frac{\partial \Phi_k}{\partial t}, \theta(h_i) \right\rangle_{Q_i} \right) + \left\{ \Phi_k, \mathcal{G}_{i\pm\frac{1}{2}} \right\}_{\partial Q_i} \\ &\quad - \langle \nabla \Phi_k, f(h_i, \nabla h_i) \rangle_{Q_i} = \left[\Phi_k, w_h^n \right]_{Q_i}^{t^n} + \langle \Phi_k, S(h_i) \rangle_{Q_i}. \end{aligned} \tag{20}$$

In (20), the term $\mathcal{G}_{i\pm\frac{1}{2}}$ is a numerical flux function depending on the left and right states h^- and h^+ and their gradients ∇h^- and ∇h^+, respectively, and is chosen according to [39] as

$$\mathcal{G}_{i\pm\frac{1}{2}} = \frac{1}{2}\left(f\left(h^+, \nabla h^+\right) + f\left(h^-, \nabla h^-\right) \right) - \frac{1}{2}\left(|\lambda_c^{\max}| + 2\eta|\lambda_v^{\max}| \right)\left(h^+ - h^-\right), \tag{21}$$

with $|\lambda_c^{\max}| = \max\left(|f_h(h^-)|, |f_h(h^+)|\right)$, $|\lambda_v^{\max}| = \max\left(|f_{\nabla h}(q^-)|, |f_{\nabla h}(q^+)|\right)$, $f_h = \partial f/\partial h$, $f_{\nabla h} = \partial f/\partial(\nabla h)$, and $\eta = \frac{1}{\Delta x}$. It is trivial to prove that the GSTDG predictor (20) conserves mass exactly. This follows directly from using $\theta_k = 1$ as the test function, which leads to a flux-difference form. Furthermore, also the final finite volume scheme (11) is exactly mass conservative, as it is directly written in flux-difference form. The GSTDG scheme (20) for RE is a high-order equivalent to the finite volume scheme presented for free surface flows in [51]. In the present case, the water content function $\theta(h)$ assumes a similar role as the volume function $V(\eta)$ in [51].

The space–time DG scheme (20) leads to a globally coupled nonlinear algebraic system solved with a Newton–Krylov method on the basis of the GMRES algorithm of Saad and Schultz [13]. Convergence of the Newton–Krylov method is improved using a classical globalization technique based on line search [52].

DOI: 10.1002/nme

3. NUMERICAL CONVERGENCE STUDIES

To assess the convergence behavior of the proposed method, we use the following relative error norm:

$$\|\theta_{\mathrm{h}} - \theta_{\mathrm{e}}\|_p = \left(\int_0^1 \left(\frac{|\theta_{\mathrm{h}}(x,t) - \theta_{\mathrm{e}}(x,t)|}{|\theta_{\mathrm{e}}(x,t)|} \right)^p \mathrm{d}x \right)^{\frac{1}{p}} \tag{22}$$

where θ_{h} denotes the numerical solution and θ_{e} the exact solution.

The error norm (22) is calculated using Gaussian quadrature rules of appropriate order of accuracy. Furthermore, we use the following error norms when comparing experimental results with numerical simulations [53]:

Absolute error

$$\mathrm{AE} = \sum_{c=1}^{d} |\theta_{\mathrm{h}} - \theta_{\mathrm{e}}|_c \tag{23}$$

Root-mean-square error (RMS)

$$\mathrm{RMS} = \sqrt{\frac{1}{d} \sum_{c=1}^{d} (\theta_{\mathrm{h}} - \theta_{\mathrm{e}})_c^2} \tag{24}$$

Logarithmic form of RMS (LRMS)

$$\mathrm{LRMS} = \sqrt{\frac{1}{d} \sum_{c=1}^{d} (\log(\theta_{\mathrm{h}}) - \log(\theta_{\mathrm{e}}))_c^2} \tag{25}$$

where c is a counter and d is the number of the experimental data, θ_{e} is the water content obtained from experimental data, and θ_{h} is the water content calculated with ADER-FV, at the same positions.

3.1. Nonlinear Richards equation

We solved the RE without source term ($S = 0$)

$$\frac{\partial \theta(h)}{\partial t} = \frac{\partial}{\partial x} \left[K(h) \frac{\partial h}{\partial x} - K(h) \right]. \tag{26}$$

The computational domain chosen in this test was $\Omega = [0; 200]$, and the following initial and boundary conditions have been specified:

$$\theta(x, 0) = 0.01,$$

$$f(0, t) = 1\,\mathrm{cm/h}, \qquad \theta(200, t) = 0.01. \tag{27}$$

The exact solution for Equation (26) was obtained in References [54, 55] on the basis of the *van Genuchten* model for the water content Equation (4) and the *Brooks–Corey* model for the hydraulic conductivity Equation (7). The following soil hydraulic parameters were used for this test case, assuming a homogeneous soil: $\alpha = 1$ cm, $\eta = 1$ and $n = 1$, $K_{\mathrm{s}} = 1$ cm/h, $\theta_{\mathrm{s}} = 0.4$, and $\theta_{\mathrm{r}} = 0.004$. The numerical convergence results obtained for the RE with the proposed ADER-FV schemes of second and third order of accuracy in space and time are shown in Table I. As before, N_{G} denotes the number of grid cells used to discretize the domain Ω. The simulation has been carried out in the time interval $t \in [10\,\mathrm{s}; 16.0837\,\mathrm{s}]$. The errors and the associated convergence rates between two successive grid refinements are shown in L^2, L^3, and L^∞ norms. The error norms are computed numerically according to Equation (22). The results presented in Table I show that the method converges with the designed order of accuracy.

DOI: 10.1002/nme

Table I. Numerical convergence rates for Richards equation ($t = 16.0837$ s) obtained with ADER-FV for second and third order of accuracy in space and time.

N_G	L^2	L^3	L^∞	O_{L^2}	O_{L^3}	O_{L^∞}
ADER-FV $\mathcal{O}2$ ($M = 2$)						
16	2.0184	1.0167	2.3494×10^{-1}			
24	9.1628×10^{-1}	4.6784×10^{-1}	1.0374×10^{-1}	1.9	1.9	2.0
32	4.7938×10^{-1}	2.4704×10^{-1}	4.9947×10^{-2}	2.3	2.2	2.5
48	1.7174×10^{-1}	8.8369×10^{-2}	2.2490×10^{-2}	2.5	2.5	2.0
56	1.2127×10^{-1}	6.2137×10^{-2}		2.3	2.3	
60	1.0839×10^{-1}	5.5748×10^{-2}	2.2490×10^{-2}	1.6	1.6	
ADER-FV $\mathcal{O}3$ ($M = 3$)						
24	9.8812×10^{-1}	5.1222×10^{-1}	1.9501×10^{-1}			
32	4.5876×10^{-1}	2.3658×10^{-1}	8.8671×10^{-2}	2.7	2.7	2.7
40	2.3054×10^{-1}	1.1714×10^{-1}	4.6010×10^{-2}	3.1	3.2	2.9
48	1.2856×10^{-1}	6.4683×10^{-2}	2.3088×10^{-2}	3.2	3.3	3.8
52	1.0371×10^{-1}	5.3401×10^{-2}		2.7	2.4	

4. NUMERICAL RESULTS

In this article, we apply the ADER-FV method of [25] to RE with stiff source term. In this article, the development of the ADER-FV method for RE with stiff source term is not considered. In order to demonstrate that the ADER-FV scheme implemented in this paper is accurate and robust, we show four different examples: column infiltration test (comparison with conventional finite element and experimental data), free drainage (comparison with conventional finite element and experimental data), comparison among finite difference, ADER-FV schemes and exact solution, and simulation with layered soil (comparison with a benchmark reference).

4.1. Column infiltration test

This example simulates a 1D laboratory infiltration experiment initially discussed by Skaggs *et al.* [56] and used for a comparison with results obtained with the HYDRUS 1D code [57]. HYDRUS 1D is a free software tool for soil simulation that uses the conventional FEM for solving RE in one space dimension [58]. The soil was assumed to be homogeneous and isotropic with a saturated hydraulic conductivity $K_s = 7.22\text{E}{-}04$ cm/s, saturated water content $\theta_s = 0.35$, and a residual water content $\theta_r = 0.02$. The parameters used for the van Genuchten model of the hydraulic conductivity were $n = 1.964$ and $\alpha = 4.1$ cm. The column was subjected to ponded infiltration (a Dirichlet boundary condition) at the soil surface, resulting in a 1D vertical water flow. The depth of the soil profile was $L = 61$ cm. The boundary and initial conditions were chosen as follows:

$$h(x,0) = -150\,\text{cm}, \quad h(0,t) = -1\,\text{cm}, \quad h(L,t) = -150\,\text{cm}. \tag{28}$$

The simulation was carried out for $t = 9000$s, which corresponds to the total temporal duration of the experiment. Meshes of 205 were used in HYDRUS 1D and 50 elements for the ADER-FV$_3$ (third order) scheme. The time step in HYDRUS 1D varied between 0.01 and 600 s. In the ADER-FV$_3$ scheme, we use a fixed time step of 600 s.

Figure 1 depicts the results obtained with the two different numerical schemes (HYDRUS 1D and ADER-FV) and the experimentally observed data. This curve is the so-called suction curve and indicates the nonlinear relation between hydraulic pressure and water content. The comparison between the numerical results and the experimental data shows that the ADER-FV$_3$ method leads to a better approximation of the experimental results for the hydraulic pressure than the HYDRUS 1D model in all the observation points. The computational time used in ADER-FV$_3$ scheme is three times higher than that the required with HYDRUS 1D.

DOI: 10.1002/nme

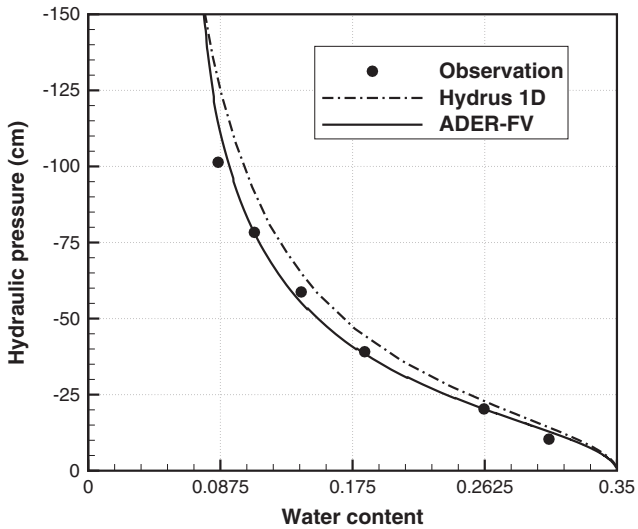

Figure 1. Comparison between numerical results (HYDRUS 1D and ADER-FV$_3$) and experimental observations for the column infiltration test.

Table II. Errors of HYDRUS 1D and ADER-FV$_3$ for the column infiltration test.

	Errors		
Method	AE	RMS	LRMS
HYDRUS 1D	58.221	1.4641	0.118
ADER-FV$_3$	19.933	9.6020E−01	0.087

The quantitative errors of both numerical methods compared with the experimental values are shown in Table II. The ADER-FV$_3$ scheme is clearly closer to the experimental results. The higher order incorporated in the algorithm allowed to increase the accuracy in the calculation of the nonlinearities produced by the flow in the unsaturated porous media.

4.2. Free drainage

The second case corresponds to a situation when the soil is drying because of natural drainage caused by gravity. Again, the numerical results are compared with those of HYDRUS 1D and experimental data. This example is provided with the HYDRUS 1D code and also may be found in References [5, 59]. In this example, the saturated hydraulic conductivity is $K_s = 25$ cm/s, the saturated water content is $\theta = 0.3308$, and the residual water content is $\theta_r = 0$. The parameters used in the hydraulic van Genuchten model are $n = 1.506$ and $\alpha = 0.01433$ cm. The experimental setup considered a caisson with a 600-cm depth and a 300-cm diameter. In HYDRUS 1D, we used 120 elements in the x direction and time steps between 4.16E−09 and 2E−02 s. To calculate the water content with ADER-FV$_3$, we used only 50 elements and a constant time step of $\Delta t = 0.1$ s. The following initial and boundary conditions, corresponding to the free drainage case, were applied:

$$h(x,0) = 0\,\text{cm}, \qquad f(0,t) = 0\,\text{cm/s}, \qquad h(L,t) = 0\,\text{cm}. \tag{29}$$

In Figure 2, numerical and experimental results are shown. Clearly, both the results obtained with HYDRUS 1D package and those calculated with the ADER-FV$_3$ scheme are in very good agreement with the experimental results. Table III shows the quantitative errors between numerical and experimental results. In days 1, 4, 20, and 100, the ADER-FV$_3$ scheme is slightly more accurate than HYDRUS 1D. Figure 2 shows that the numerical results are more accurate when the system tends to balance the steady state. In this test, the computational time for the calculations with the

DOI: 10.1002/nme

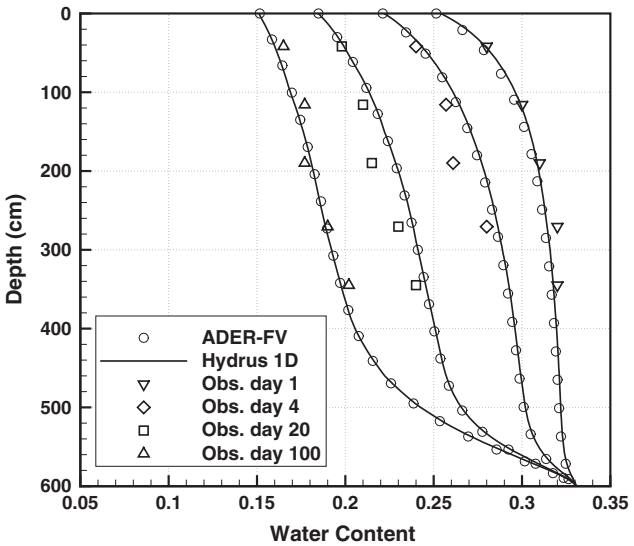

Figure 2. Comparison between numerical results (HYDRUS 1D and ADER-FV$_3$) and experimental values for the free drainage test case.

Table III. Errors of HYDRUS 1D and ADER-FV$_3$ compared with observed data for the free drainage test case.

	Program					
	HYDRUS 1D			ADER-FV$_3$		
	AE	RMS	LRMS	AE	RMS	LRMS
Day 1	1.1482E−02	2.2941E−02	2.6942E−02	2.1234E−02	4.1318E−02	3.4119E−02
Day 4	4.5226E−02	4.3271E−02	5.4532E−02	3.9657E−02	4.0960E−02	5.1666E−02
Day 20	3.4870E−02	3.8522E−02	5.3569E−02	3.3428E−02	3.7751E−02	5.2525E−02
Day 100	2.0367E−02	2.8260E−02	4.4405E−02	1.9432E−02	2.7763E−02	4.3489E−02

ADER-FV$_3$ scheme is similar to the one needed by the HYDRUS 1D code; the higher-order scheme can produce accurate results with a lower number of cells and a larger time step.

4.3. Comparison between finite difference and ADER-FV schemes

In this case, we compare an exact solution of RE with the numerical results obtained with an FD scheme [55] and the ADER-FV$_3$ method developed in this article. The FD program uses an adaptive, second-order diagonally implicit Runge–Kutta time-stepping method and the Newton method with simple Jacobian of lagged intergrid conductivities and a mixed water-content/head formulation of RE. The FD program uses a simple version of Darcian intergrid conductivity means [54]. To calculate the hydraulic properties, we used the van Genuchten model for the water content Equation (4) and the Brooks–Corey model for the hydraulic conductivity, as stated by Equation (7). The soil hydraulic parameters used in these models are $\alpha = 1$ cm, $\eta = 2$, $n = 1$, $K_s = 1$ cm/h, $\theta_s = 0.4$, and $\theta_r = 0.004$. Two meshes of 100 and 800 nodes were used for the finite difference scheme to ensure convergence of the solution. A variable time step between 1E−06 and 1 h has been used for the finite difference scheme, and a constant time step of $\Delta t = 2E$-01 h was used for the ADER-FV$_3$ method. The initial and boundary conditions are

$$\theta(x,0) = 0.01, \qquad f(0,t) = 1\ \text{cm/h}, \qquad \theta(L,t) = 0.01. \tag{30}$$

In Figure 3, the variation of water content with depth calculated using the exact solution is compared with the results obtained with the finite difference scheme and the ADER-FV$_3$ method. The 800 nodes FD solution obviously does *not* converge to the exact solution. Finite difference programs

DOI: 10.1002/nme

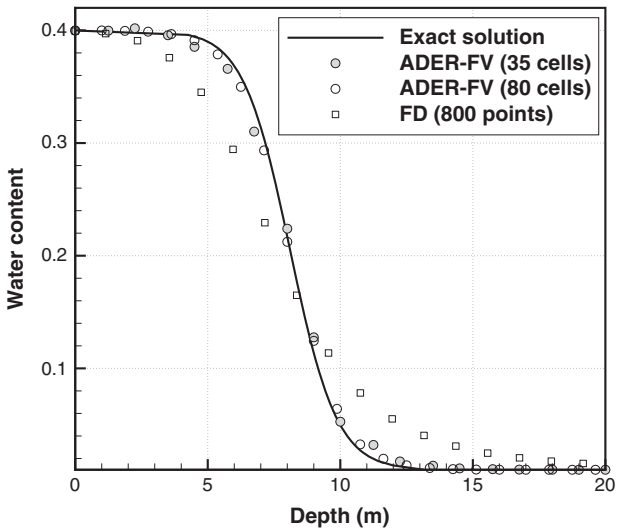

Figure 3. Comparison between exact and numerical solutions (FD and ADER-FV_3) for test case 4.3.

Table IV. Hydraulic parameters for soil 1 and 2 (case 4.4).

	Soil 1	Soil 2
θ_s	0.3658	0.4686
θ_r	0.0286	0.1060
α (1/m)	2.80	1.04
n	2.2390	1.3954
K_s (m/s)	6.26E−05	1.5161E−06

only work well if the changes in variables and their derivatives between grid points are not too extreme. The extremely sharp nature of the wetting front has prevented the scheme from converging to a solution. However, we observe that using the ADER-FV_3 method with only 35 elements already shows a rather good approximation. The accuracy of ADER-FV_3 method shows a minor improvement when the mesh is refined to 80 elements.

This test shows that the ADER-FV schemes tends to the RE exact solution.

4.4. Simulation with layered soil

The exact solutions for RE in 1D are restricted to simple boundary conditions with one soil type; hence, a test with layered soil is included for testing the ADER-FV scheme. This last test case corresponds to a layered soil profile and has been used as a benchmark by several authors [10, 60–62] to verify semi-analytical and numerical solutions. The hydraulic parameters of the two soils used for the model are summarized in Table IV. Soil 1 and 2 are Berino loamy fine sand and Glendale clay loam, respectively [62]. The soil profile contains soil 1 in the intervals [0;0.5 m] and [0.9;1 m], respectively, and soil 2 from 0.5 to 0.9 m. The van Genuchten model is used to describe the hydraulic properties. The simulation time and initial and boundary conditions are given in Table V. Calculations with the ADER-FV_2 and ADER-FV_3 schemes were accomplished by using a mesh with 50 elements and time step that changed from 50 to 100 s.

Figure 4 shows the results obtained with ADER-FV schemes for both water content and pressure head changes for unsaturated flow in layered soil. The results are in good agreement with the ones published in the literature [10, 60]. The good results obtained in this test show that ADER-FV schemes developed in this work may be easily used to describe water motion, from the nonlinear RE, in unsaturated porous media in layered soils. The numerical approach presented in this paper

DOI: 10.1002/nme

Table V. Initial and boundary conditions, simulation times (case 4.4).

Case	Initial pressure (m)	Upper flux (m/s)	Lower boundary (m/s)	Simulation time (s)
1	−2	8.333E−07	0.0	14,400
2	−10	8.333E−07	0.0	28,800
3	−500	8.333E−07	0.0	43,200

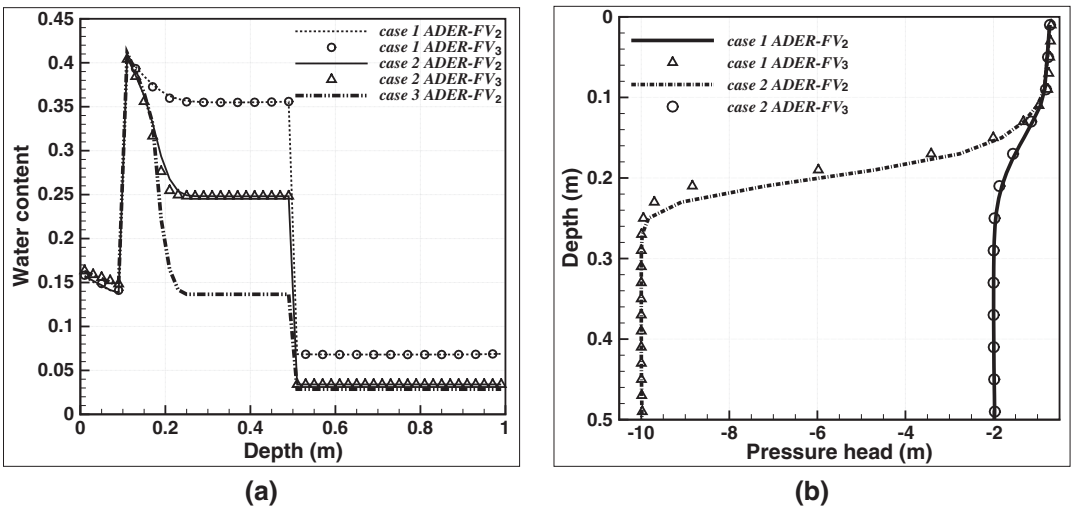

Figure 4. ADER-FV results for (a) volumetric water content versus depth, cases 1–3, and (b) pressure head versus depth, cases 1 and 2.

can be extended to 2D and 3D problems. One of the main expected advantages would be high increments in the accuracy of the solutions that should require much higher computation time than the available procedures as a drawback.

5. SUMMARY AND CONCLUSION

We have developed a new explicit unsplit ENO finite volume scheme of high order of accuracy in space and time for the nonlinear RE. We emphasize that the discontinuous Galerkin scheme used is globally implicit but is only a part of the complete algorithm, a predictor, in fact. The global scheme is an explicit finite volume scheme (11). The spatial reconstruction polynomials obtained from the WENO reconstruction operator are used as initial conditions for the GSTDG predictor scheme. The predictor solution for the hydraulic pressure is then used in the final finite volume method to update the cell averages of the water content. The resulting scheme is *exactly* mass conservative, as it is directly written in flux-difference form for the water content. In this article, we use a Newton–Krylov method based on the GMRES algorithm of Saad and Schultz [13] to solve the resulting non-symmetric linear subsystems arising in the Newton algorithm. Numerical test cases show that the proposed ADER-FV schemes do not only reach their designed order of accuracy, but that they are also superior to classical finite difference schemes, which may fail to converge to the exact solution of RE.

ACKNOWLEDGEMENTS

This study was funded by the Publishing Arts Research Council (98-1846389). The authors thank CONICYT for financial support to FONDECYT 1111067 project and the Italian Ministry of Research and University (MIUR) for financial support under the PRIN 2007 project.

DOI: 10.1002/nme

REFERENCES

1. Richards LA. Capillary conduction of liquids through porous mediums. *Physics* 1931; **1**:318–333.
2. Mansell RS, Liwang M, Ahuja LR, Bloom SA. Adaptative grid refinement in numerical models for water flow and chemical transport in soil: a review. *Vadose Zone Journal* 2002; **1**:222–238.
3. Milly PCD. A mass-conservative procedure for time-stepping in models of unsaturated flow. *Advances in Water Resources* 1985; **8**:32–36.
4. Celia MA, Bouloutas ET, Zarba RL. A mass-conservative numerical solution for unsaturated flow equation. *Water Resources Research* 1990; **26**:1483–1496.
5. Forsyth PA, Wu YS, Pruess K. Robust numerical methods for saturated–unsaturated flow with dry initial conditions in heterogeneous media. *Advances in Water Resources* 1995; **18**:25–38.
6. Kavetski D, Binning P, Sloan SW. Adaptative backward Euler time stepping with truncation error control for numerical modelling of unsaturated fluid flow. *International Journal for Numerical Methods in Engineering* 2001; **53**:1301–1322.
7. Li H, Farthing MW, Dawson CN, Miller CT. Local discontinuous Galerkin approximation to Richards equation. *Advances in Water Resources* 2007; **30**(3):555–575.
8. Li H, Farthing MW, Miller CT. Local discontinuous Galerkin approximation to Richards equation. *Advances in Water Resources* 2007; **30**(9):1883–1991.
9. Ju SH, Kung KJS. Mass types, elements orders and solution schemes for Richards equation. *Computers & Geosciences* 1997; **23**:175–187.
10. McBride D, Cross M, Croft N, Bennett C, Gebhardt J. Computational modelling of variably saturated flows in porous media with complex three-dimensional geometries. *International Journal for Numerical Methods in Fluids* 2006; **50**:1085–1117.
11. Eymard R, Gutnic M, Hilhorst D. The finite volume method for the Richards equation. *Computers and Geosciences* 2000; **3**(3–4):259–294.
12. Manzini G, Ferraris S. Mass-conservative finite volume methods on 2-D unstructured grids for the Richards equation. *Advances in Water Resources* 2004; **27**(12):1199–1215.
13. Saad Y, Schultz MH. GMRES: a generalized minimal residual algorithm for solving nonsymmetric linear systems. *Journal on Scientific and Statistical Computing* 1986; **7**(3):856–869.
14. Fassino C, Manzini G. Fast-secant algorithms for non-linear Richards equation. *Communications in Numerical Methods in Engineering* 1998; **14**:921–930.
15. Bergamaschi L, Putti M. Mixed finite elements and Newton-type linearizations for the solution of Richards equation. *International Journal for Numerical Methods in Engineering* 1999; **45**:1025–1046.
16. Kavetski D, Binning P, Sloan SW. Noniterative time stepping schemes with adaptative truncation error control for the solution of Richards equation. *Advances in Water Resources* 2002; **24**:595–605.
17. Brooks RH, Corey AT. Hydraulic Properties of Porous Media. *Hydrology, Civil Engineering, Colorado State University* 1964; Paper No. 3.
18. Van Genuchten MT. A closed form equation for predicting the hydraulic conductivity of unsaturated soils. *Soil Science Society of American Journal* 1980; **44**:892–898.
19. Vogel T, van Genuchten MT, Cislerová M. Effect of the shape of the soil hydraulic functions near saturation on variably-saturated flow predictions. *Advances in Water Resources* 2001; **24**(2):133–144.
20. Vogel T, Cislerová M. On the reliability of unsaturated hydraulic conductivity calculated from the moisture retention curve. *Transport in Porous Media* 1988; **3**:1–15.
21. Kosugi K. Lognormal distribution model for unsaturated soil hydraulic properties. *Transport in Porous Media* 1996; **32**(9):2697–2703.
22. Durner W. Hydraulic conductivity estimation for soils with heterogeneous pore structure. *Water Resources Research* 1994; **32**(9):211–223.
23. Mualem Y. A new model for predicting the hydraulic conductivity of unsaturated porous media. *Water Resources Research* 1976; **12**:513–522.
24. Harten A, Engquist B, Osher S, Chakravarthy S. Uniformly high order essentially non-oscillatory schemes, III. *Journal of Computational Physics* 1987; **71**:231–303.
25. Dumbser MC, Enaux, Toro EF. Finite volume schemes of very high order of accuracy for stiff hyperbolic balance laws. *Journal of Computational Physics* 2008; **227**(8):3971–4001.
26. Dumbser M, Balsara D, Toro ET, Munz CD. A unified framework for the construction of one-step finite-volume and discontinuous Galerkin schemes. *Journal of Computational Physics* 2008; **227**:8209–8253.
27. Toro EF, Titarev VA. Solution of the generalized Riemann problem for advection–reaction equations. *Proceedings Of The Royal Society Of London Series A-Mathematical Physical And Engineering Sciences* 2002; **458**:271–281.
28. Titarev VA, Toro EF. ADER schemes for three-dimensional nonlinear hyperbolic systems. *Journal of Computational Physics* 2005; **204**(2):715–736.
29. Van der Vegt JJW, van der Ven H. Space–time discontinuous Galerkin finite element method with dynamic grid motion for inviscid compressible flows I. General formulation. *Journal of Computational Physics* 2002; **182**(2):546–585.
30. Van der Ven H, van der Vegt JJM. Space–time discontinuous Galerkin finite element method with dynamic grid motion for inviscid compressible flows II. Efficient flux quadrature. *Computer Methods in Applied Mechanics and Engineering* 2002; **191**:4747–4780.

DOI: 10.1002/nme

31. Godunov SK. Finite difference methods for the computation of discontinuous solutions of the equations of fluid dynamics. *Mathematics of the USSR* 1959; **47**:271–306.
32. Engquist B, Osher S. One side difference approximations for nonlinear conservation laws. *Mathematics of Computation* 1981; **36**:321–351.
33. Roe PL. Approximate Riemann solvers, parameter vectors, and difference schemes. *Journal of Computational Physics* 1981; **43**:357–372.
34. Harten A, Lax PD, van Leer B. On upstream differencing and Godunov-type schemes for hyperbolic conservation laws. *SIAM Review* 1983; **25**(1):35–61.
35. Einfeldt B. On Godunov-type methods for gas dynamics. *SIAM Journal on Numerical Analysis* 1988; **25**(1):294–318.
36. Einfeldt B, Munz CD, Roe PL, Sjgreen B. On Godunov-type methods near low densities. *Journal of Computational Physical* 1991; **92**:273–295.
37. Toro EF, Spruce M, Speares W. Restoration of the contact surface in the Harten-lax-van Leer Riemann solver. *Journal of Shock Waves* 1994; **4**:25–34.
38. Toro EF. *Riemann Solvers and Numerical Methods for Fluid Dynamics*, 3rd ed. Springer Verlag, 2009.
39. Dumbser M. Arbitrary high order PNPM schemes on unstructured meshes for the compressible Navier–Stokes equations. *Computers & Fluids* 2010; **39**:60–76.
40. Dumbser M, Munz CD. Building blocks for arbitrary high order discontinuous Galerkin schemes. *Journal of Scientific Computing* 2006; **27**:215–230.
41. Dumbser M, Käser M, Titarev VA, Toro ET. Quadrature-free non-oscillatory finite volume schemes on unstructured meshes for nonlinear hyperbolic systems. *Journal of Computational Physics* 2007; **226**:204–243.
42. Arnold D, Brezzi F, Cockburn B, Marini D. Unified analysis of discontinuous Galerkin methods for elliptic problems. *SIAM Journal of Numerical Analysis* 2002; **39**:1749–1779.
43. Cockburn B. Discontinuous Galerkin methods for convection-dominated problems. *Lecture Notes in Computer Science and Engineering* 1999; **9**:69–224.
44. Cockburn B. Discontinuous Galerkin methods. *ZAMM-Journal of Applied Mathematics and Mechanics* 2003; **11**:731–754.
45. Cockburn B, Shu CW. Runge–Kutta discontinuous Galerkin methods for convection-dominated problems. *Journal of Science and Computation* 2001; **16**:173–261.
46. Klaij CM, van der Vegt JJW, van der Ven H. Space–time discontinuous Galerkin methods for the compressible Navier–Stokes equations. *Journal of Computational Physics* 2006; **16**:589–611.
47. Van der Vegt J, Xu Y. Space–time discontinuous Galerkin methods for nonlinear water waves. *Journal of Computational Physics* 2007; **224**(1):17–39.
48. Dumbser M, Käser M. Arbitrary high order non-oscillatory finite volume schemes on unstructured meshes for linear hyperbolic systems. *Journal of Computational Physics* 2007; **221**:693–723.
49. Jiang GS, Shu CW. Efficient implementation of weighted ENO schemes. *Journal of Computational Physics* 1996; **126**:202–228.
50. Liu XD, Osher S, Chan T. Weighted essentially non-oscillatory schemes. *Journal of Computational Physics* 1994; **115**:200–212.
51. Casulli V. A high-resolution wetting and drying algorithm for free-surface hydrodynamics. *International Journal for Numerical Methods in Fluids* 2009; **60**:391–408.
52. Press WH, Teukolsky SA, Vetterling WT, Flannery BP. *Numerical Recipes in Fortran 77*, Vol. 1. Cambridge University Press, 1996.
53. Abbaspour KC, van Genuchten MT, Schulin R, Schlappi E. A sequential uncertainty domain inverse procedure for estimating subsurface flow and transport parameters. *Water Resources Research* 1997; **33**(8):1879–1892.
54. Baker DL, Arnold ME, Scott HD. Some analytical and approximate Darcian means. *Ground Water* 1999; **37**(4):532–538.
55. A quasi-analytic general solution of Richards equation for vertical unsaturated flow in homogeneous media with constant inflow. http://www.aquarien.com/gsreq/index.html [24 September 2010].
56. Skaggs RW, Monke EJ, Huggins LF. *An Approximate Method for Determining the Hydraulic Conductivity Function of an Unsaturated Soil*. Water Resource Research Center, Purdue University: Lafayette, 1970.
57. Simunek J, van Genuchten MT, Sejna M. *The Hydrus-1D Software Package for Simulating the One-Dimensional Movement of water, Heat and Multiple Solutes in Variably-Saturated Media*. Department of Environmental Science University of California Riverside: Riverside California, 2005.
58. Hydrus-1D. Selected References. http://www.pc-progress.com/en/Default.aspx?h1d-references [24 September 2010].
59. Kool J, van Genuchten MT. HYDRUS. A One Dimensional Variably Saturated Flow and Transport Model, Including Hysteresis and Root Water Uptake, Version 3.3. *US Salinity Laboratory Technical Report*, US Department of Agriculture, Riverside California, 1991.
60. Pan L, Wierenga PJ. A transformed pressure head-based approach to solve Richards equation for variably saturated soil. *Water Resources Research* 1995; **31**(4):925–931.
61. Kirkland MR, Hills RG, WierengaM P J. Algorithms for solving Richards equation for variably saturated soils. *Water Resources Research* 1992; **28**:2049–2058.
62. Hills RG, Porro I, Hudson DB, Wierenga PJ. Modeling one-dimensional infiltration into very dry soils. 1. Model development and evaluation. *Water Resources Research* 1989; **25**:1259–1269.

DOI: 10.1002/nme